# VISUAL QUALITY AND ILLUMINATION ENHANCEMENT USING GAMMA CORRECTED GAUSSIAN FILTERING FRAMEWORK FOR COVID-19 IMAGES

## Duraiswamy Umamaheswari[1] and Shanmugam Geetha[2]

*[1]Department of Computer Science, Government Arts College, Udumalpet, India*
*[2]Department of Computer Science, LRG Government Arts College for Women, India*

*Abstract*

*The initiation tasks of Digital image processing (DIP), the image enhancement techniques are used to better represent the image content and make them ready for further analysis. The pre-processed images can be easily handled by the successive steps of DIP such as image sharpening, image restoration, image segmentation, and object recognition. An image is fabricated with the basic picture elements referred to as pixels. Noisy pixels create distortion in the image and that can be suppressed and smoothened using image pre-processing tasks. Bundles of standard preprocessing techniques are there in the field. A framework named Gamma Corrected Gaussian Filtering (GCGF) is proposed in this article for reducing the noise produced by radiographic or Computed Tomography (CT) machines and enhancing the luminance of the captured images by applying histogram equalization and Gaussian filter followed by Gamma correction. The standard image filtering methods such as Mean filter, Weighted-Averaging filter, Minimum filter, Maximum filter, Wiener filter, Median filter, along with Gaussian filter are discussed and compared with the proposed Gamma Corrected Gaussian Filtering (GCGF) framework through the metrics Mean Square Error (MSE) and Peak Signal to Noise Ratio (PSNR) using the chest X-ray dataset of COVID-19 patients.*

*Keywords:*

*Filtering, Image Processing, Gamma, Gaussian, Preprocessing*

## 1. INTRODUCTION

DIP is a vast domain assists to process the images by means of applying evolving techniques and tools. The major tasks of DIP are image acquisition, pre-processing, segmentation, and post-processing. The Pre-processing methods facilitate in filtering the noise and enhancing the illumination, contrast, and overall content of the digital images. In recent years, Machine Learning (ML) and Deep Learning (DL) are giving their best in the medical and healthcare sectors to disease diagnosis. Meaningful features paw the way for the most accurate diagnosis. For delivering healthier images to acquire meaningful features, efficient pre-processing techniques are mandatory [1] [2].

The medical images are acquired through the imaging systems such as MRI scan, CT scan, X-rays, and Microscopes [3] [4]. The image capturing systems capture the tissues, blood flow, organs, bones, and other particles of the body which may be continuous in motion. Hence, the received image may contain diverse type noises like salt and pepper noise, speckle noise, Gaussian noise, and Poisson noise [5]. As a result, the image pixels are depicted in different intensity ranges. These inaccurate and noisy images cannot give obvious details for further analysis. Due to this reason, preprocessing is getting into the picture to play its role in enhancing the images. Image enhancement techniques are actually lower level image processing techniques. One such image enrichment technique is known as filtering.

The proposed Gamma Corrected Gaussian Filtering (GCGF) framework is specifically meant for smoothing the X-ray and CT scan images with photonic noise produced by the imaging devices. The radiographic machines make noise on situations when there is some variation found in radio signals. The variation in X-ray is caused by the increased or reduced range of radiation than the prescribed level. The change in radiation causes fluctuations in the X-ray images; which are referred to as quantum noise. Quantum noises occur randomly all over the image. This noise can be cleared by doing the appropriate level of Gamma correction on the image.

Silpasai et al. [6] used gamma correction along with the Cuckoo search optimizer for enhancing the luminance of the histopathological images. The selected input image is converted to HSV color space and then Gaussian filter is applied. Illumination adjustment of the filtered image is done by Gamma correction alone, and then cuckoo search optimizer is applied for intensity optimization. Singh et al. [7] also did Gamma correction along with histogram equalization for increasing the illumination of low light satellite images. Contrast adjustment of the illumination adjusted images is done by applying swarm optimizer. Suman et al. [8] used the geometric mean filter with Gamma correction for enhancing the quality of Wireless capsule Endoscopy images. The Algorithm is assessed using the evaluation metrics SNR and PSNR.

In this article, spatial domain filters are examined for knowing their impact on the reduction of quantum noise present in chest X-ray images. The proposed GCGF framework uses histogram equalization for normalizing the intensity of the image and Gamma correction for improvising the visual quality of the image. The operational competences of the standard and proposed filtering methods are evaluated through their MSE and PSNR values by applying the filters to 25 sample images.

## 2. FILTERING TECHNIQUES

In the image processing arena, different sorts of filtering methods have been developed. These filtering methods are widely categorized into two types:

### 2.1 LOW-PASS FILTERS

Low-Pass filters are also referred to as image smoothing filters. They reduce noise and give visually good images for extracting more information from data. This is done by reducing the intensity values of each and every individual pixel according to its neighboring pixels. Low-Pass filters are sometimes referred to as averaging filters since they give the average intensity value of neighborhood pixels [9].

### 2.2 HIGH-PASS FILTERS

These are the filters otherwise called as image sharpening methods, as they increase the quality of the image by providing additional details. The main goal of High-Pass filters is to emphasize the changes in intensity [10].

Both low-pass as well as high-pass filter can be used in both frequency and spatial domains.

## 3. SPATIAL DOMAIN SMOOTHING FILTERS

Smoothing (low-pass) and sharpening (high-pass) filters are further categorized either as spatial domain filters or frequency domain filters. The spatial domain filters filter the noise in images by making changes in the intensity values of the target pixels based on their nearby or neighboring pixels. Spatial domain is easy to understand because they directly work on pixels. The basic functioning of spatial domain filters is expressed as:

$$T(x,y) = P(f(x,y)) \qquad (1)$$

where, $T(x,y)$ is the resulting image, $P$ is the operator applied on the image, $f(x,y)$ represents the source image.

### 3.1 LINEAR SMOOTHING FILTERS

#### 3.1.1 Mean Filter (Average Filter):

This is a simple linear smoothing filter for reducing the noise of an image by adjusting the intensity of the pixels based on the intensities of their neighboring pixels. Mean filter works on replacing the intensity value of a sample pixel, with the average intensity assessment calculated on its adjacent pixels including itself. Fundamentally the mean filter functions by using a 3×3 convolution kernel [11]. As of the need, 5×5 square kernels and more than that can also be used. Notational representation of the mean filter is:

$$T(x, y) = \frac{1}{mn} \sum_{u,v \in S_{xy}} g(u,v) \qquad (2)$$

where, $T(x,y)$ is the filtered image and $g(u,v)$ is the source image.

The Fig.1 shows the convolution window of the mean filter.

| 1/9 | 1/9 | 1/9 |
|-----|-----|-----|
| 1/9 | 1/9 | 1/9 |
| 1/9 | 1/9 | 1/9 |

Fig.1. A 3×3 Convolution Kernel of Average Filter

#### 3.1.2 Weighted-Averaging Filter:

Weighted-averaging filter works on multiplying pixels falling within the selected window size by varying coefficient values of the kernel. The typical convolutional kernel size is 3×3. The image pixel which is coming at the center of the selected window is multiplied by the highest value of the kernel. The Fig.2 shows the convolutional kernel of the weighted-average filter.

| 1/16 | 2/16 | 1/16 |
|------|------|------|
| 2/16 | 4/16 | 2/16 |
| 1/16 | 2/16 | 1/16 |

Fig.2. A 3×3 Convolution Kernel of Weighted-Averaging Filter

### 3.2 NON-LINEAR SMOOTHING FILTERS (ORDER STATISTICAL FILTERS)

#### 3.2.1 Minimum Filter:

The target pixel is reimbursed by the smallest value of the selected window of the image. The minimum filter is also called as an erosion filter. The minimum filter is described as:

$$T(x, y) = \min_{u,v \in S_{xy}} g(u,v) \qquad (3)$$

#### 3.2.2 Maximum Filter:

The target pixel is reimbursed by the highest value of the selected window of the image. Maximum filter is also referred to as dilation filter. The maximum filter is represented as:

$$T(x, y) = \max_{u,v \in S_{xy}} g(u,v) \qquad (4)$$

#### 3.2.3 Median Filter:

This nonlinear smoothing median filter produces better results than mean filters. The cause behind this is median filters are not blindly replacing a pixel by the average of its neighbors, instead, it sorts all the bordering pixels' intensity values including itself, and takes the median value amongst them. The median filtering is the most widespread method because it cares for the edges [12].

$$T(x, y) = \underset{u,v \in S_{xy}}{\text{median}}\, g(u,v) \qquad (5)$$

## 4. FREQUENCY DOMAIN SMOOTHING FILTERS

Frequency domain filters work depending on the frequency of occurrence of a particular pixel. They make changes on the pixels' Fourier transform for clearing the noise. Fourier transformation is performed on the source image and is multiplied with the filter; the resulting image is given for performing reverse Fourier transformation. This process yields the noise cleared image.

### 4.1 LINEAR SMOOTHING FILTERS

#### 4.1.1 Gaussian Filter:

The Gaussian linear filter smoothens the image by making changes to the neighborhood pixels. As sticking with the category it comes under, this frequency-domain smoothing filter reduces the noise in the given image and smoothens it by applying the Gaussian function for doing convolution [13].

#### 4.1.2 Wiener Filter:

This is also a linear smoothing filter usually used in the frequency domain. Wiener filter is represented as:

$$W(u,v) = \frac{H(u,v)}{|H(u,v)|^2 + S_{nx}(u,v)} \quad (6)$$

where, $S_{nx}(u,v)$ represents the signal-to-noise-ratio (SNR), $H(u,v)$ depicts the sinc function of the target pixel. It overturns the blurring effects by multiplying the Fourier transform of the noisy image with Wiener filter [14].

## 5. PROPOSED METHODOLOGY

The input images are the X-rays and CT scans fetched from chest X-ray dataset. This dataset has images of divergent resolution ranges. Though the existing and proposed filtering techniques are able to process such images, their efficacy cannot be compared at certain circumstances. Therefore, the input images are resized to a common size of 256 pixels width and 256 pixels height [15].

Some of the images in the dataset are in three dimensions. For that reason all images are converted to grayscale before proceeding histogram equalization. Before filtering the image and adjusting the illumination, the intensity adjustment is done with the application of the histogram equalization process. By normalizing the intensity of pixels, the histogram equalization enhances the contrast of the X-ray images [16]. The histogram equalization of the input image $I$ is represented as:

$$h_n = \frac{\text{Number of Pixels with Intensity } n}{\text{Total Number of pixels in the Image}} \quad (7)$$

The intensity value of the image pixels is falling in between 0 to $L$-1. Hence, n is in the range of 0,1,…,$L$-1.

After applying the histogram equalization, the equalized X-ray image is represented as:

$$J_{x,y} = floor(L-1)\sum_{n=0}^{I_{x,y}} h_n \quad (8)$$

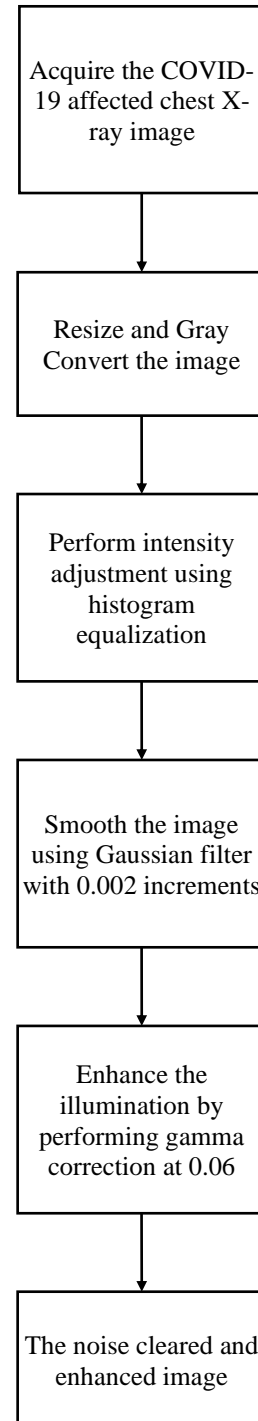The Fig.3 describes the steps involved in the proposed Gamma Corrected Gaussian Filtering framework.



Fig.3. Workflow of Proposed GCGF Framework

2256

After doing intensity adjustment using histograms the Gaussian filter is applied. Gaussian image enhancement is done by applying a suitable Gaussian convolution kernel. Finding the appropriate convolutional kernel plays crucial role in preprocessing the X-ray images. Gaussian filter's convolution kernel looks like a Gaussian hump. It is notationally represented as:

$$G(x, y) = \frac{1}{\sqrt{2\pi}\sigma} e^{-\frac{x^2 + y^2}{2\sigma^2}} \qquad (9)$$

Here, the standard deviation $\sigma$ describes the pixel distribution. The Fig.4 shows a sample Gaussian kernel with increment is done on 0.001 frequencies.

| 1/273 | 4/273 | 7/273 | 4/273 | 1/273 |
|-------|-------|-------|-------|-------|
| 4/273 | 16/273 | 26/273 | 16/273 | 4/273 |
| 7/273 | 26/273 | 41/273 | 26/273 | 7/273 |
| 4/273 | 16/273 | 26/273 | 16/273 | 4/273 |
| 1/273 | 4/273 | 7/273 | 4/273 | 1/273 |

Fig.4. Sample Gaussian Filter

Gaussian filter finds the weighted mean of the neighborhood pixels; the average is highly weighted towards the center pixels. The Gaussian filter provides high-frequency response to all the pixels of the selected region; hence, it tenderly enhances or smoothens the image based on the standard deviation value of Gaussian. Because of this reason Gaussian filters operate better than other convolution filters against the photonic noise created by the medical image capturing devices. The proposed GCGF framework does the Gaussian increment in the rate of 0.002. Followed by the Gaussian filtering, Gamma adjustment is performed.

Gamma correction is needed to medical image datasets containing images taken on different circumstances using different imaging devices and on different lightings. As the Corona pandemic made an abnormal condition in hospitals and laboratories, the chest X-ray image data set contains images of COVID-19 affected patients in varying luminance (brightness) levels. The luminance fabricated by the medical image capturing devices is not linear; they are proportional to the voltage given to the machine. Using Gamma correction the non-linear luminance of images can be adjusted to higher or lower range.

The Gamma correction is done in between the values zero and one. Zero (0) depicts complete black and one (1) depicts complete white. The Gamma correction is done for the test dataset towards one. The function for Gamma correction is represented in shorter notation as:

$$I_{OUT} = A \cdot I_{IN}^{\gamma} \qquad (10)$$

where, $I_{OUT}$ is the output produced after Gamma correction. $I_{IN}$ is the input and which is increased to the power $\gamma$. A is the constant ranges between zero and one. For the chosen COVID-19 chest X-ray images the Gamma correction is performed at the rate of 0.06. The GCGF framework ensures its novelty by choosing appropriate Gaussian kernel increment and Gamma correction constant.

## 6. EXPERIMENTS AND RESULTS

The existing and proposed filters have been tested with Chest X-ray dataset [17]. The dataset contains 760 X-ray and CT images. Out of them, randomly chosen 25 images are taken for the experiment. The dataset contains images of varying intensities like 568×492, 773×768 and 428×360.

The Fig.5 shows the input image, resized image, and noisy image. The resized noisy image is fed to the existing filters and proposed filtering technique.
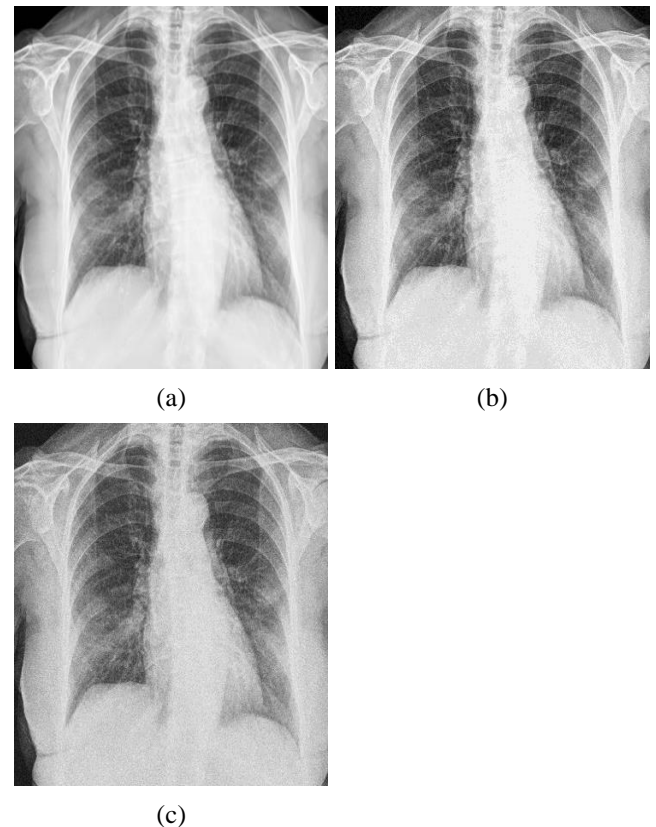


(a)                    (b)



(c)

Fig.5. Input: (a) Original Image (b) Resized and Gray Converted Image (c) Noisy Image

This huge dataset is especially helpful for pursuing deep learning-based researches. But the images are taken on various circumstances, and with different lighting. The varying circumstances make dissimilarity in the resolution of the images

and pre-processing as an essential task before submitting the images to any other algorithms. For the purpose of finding the efficiency of the existing and proposed filters through the common evaluation metrics, the feed images are resized to get standard size images.

The results of the existing filters and the proposed methodology are presented in Fig.6.



(a)　　　　　　　　(b)



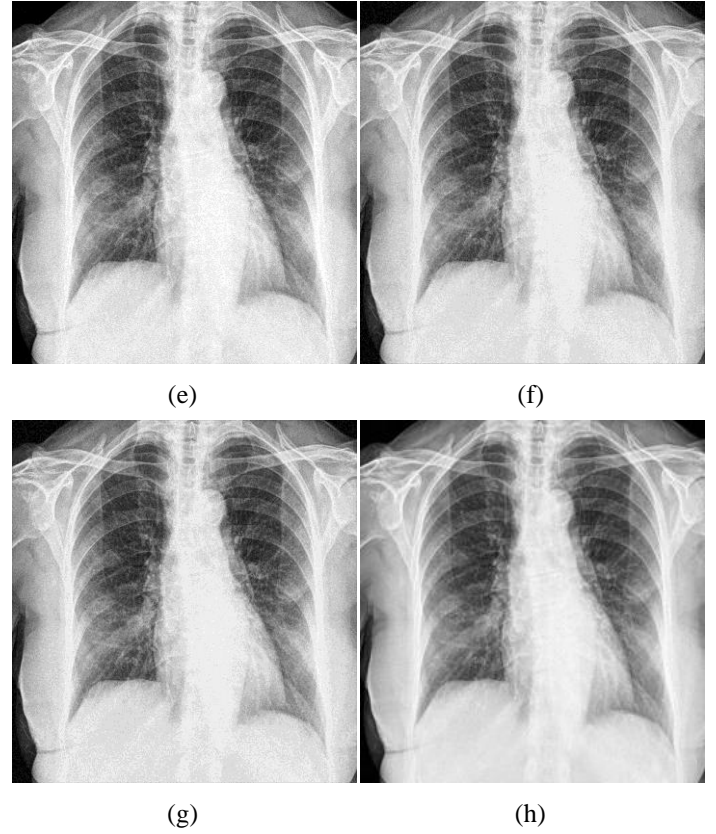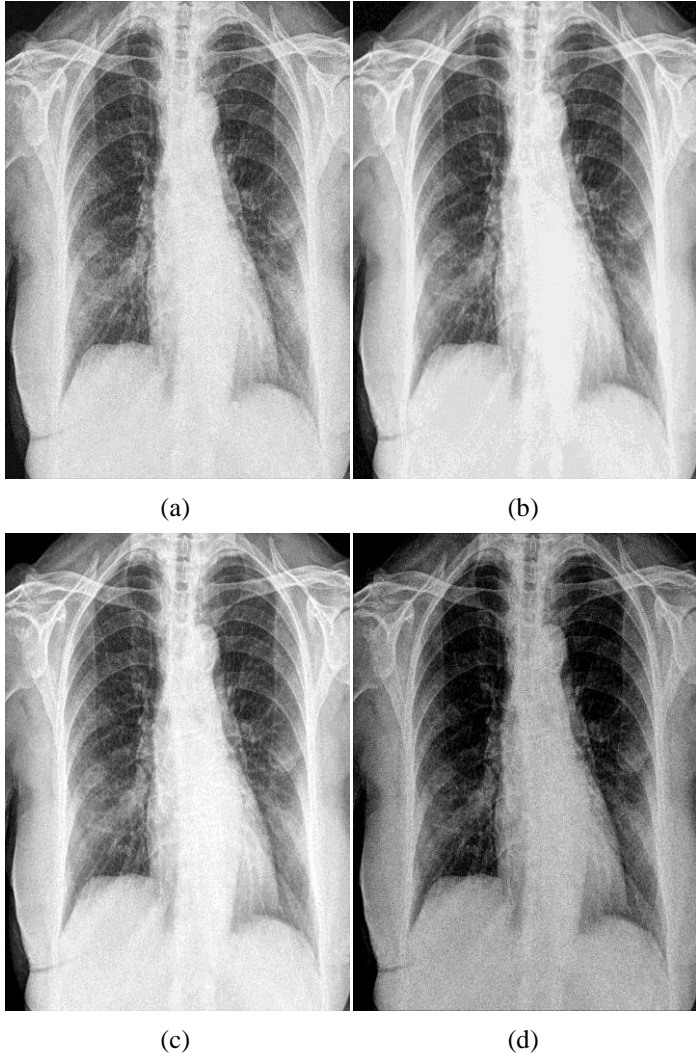(c)　　　　　　　　(d)



(e)　　　　　　　　(f)



(g)　　　　　　　　(h)

Fig.6. Processed Images of (a) Mean Filter, (b) Weighted-Averaging Filter (c) Gaussian Filter (d) Minimum Filter (e) Maximum Filter (f) Median Filter (g) Wiener Filter (h) Proposed Gamma Corrected Gaussian Filter

The pre-processing filters can be evaluated using a number of methods. In this proposal, MSE and PSNR are used as the performance evaluation measures. An image is thought to contain good quality, if it has a low amount of errors. Therefore, MSE value must be lesser for the output image that obtained from the filters. The formula for Mean Square Error is defined as [18]:

$$MSE = \frac{1}{MN} \sum_{y=1}^{M} \sum_{x=1}^{N} \left[ I(x, y) - I'(x, y) \right] \quad (11)$$

For the fine quality of the image, the PSNR value has to be larger for the objective image. PSNR value is represented as [19] [20]:

$$PSNR = 20\log_{10} \frac{255}{\sqrt{MSE}} \quad (12)$$

Table.1. Mean Square Error of the Proposed Gamma Corrected Gaussian Filtering Framework and the Traditional Filters

| Sample Image | MSE of Existing Spatial Domain and frequency Domain Filters | | | | | | | MSE of Proposed Filter |
| | Mean Filter | Weighted Averaging Filter | Minimum Filter | Maximum Filter | Median filter | Wiener Filter | Gaussian Filter | |
|---|---|---|---|---|---|---|---|---|
| Image1 | 585.33 | 562.41 | 605.21 | 515.24 | 567.14 | 575.13 | 418.66 | 214.66 |
| Image2 | 526.14 | 478.40 | 552.43 | 453.33 | 463.26 | 407.48 | 376.90 | 223.31 |
| Image3 | 574.49 | 564.35 | 586.22 | 510.28 | 581.85 | 522.36 | 409.60 | 188.14 |
| Image4 | 579.34 | 551.87 | 605.23 | 496.50 | 524.43 | 473.93 | 415.17 | 201.17 |
| Image5 | 731.03 | 571.69 | 840.80 | 601.0 | 601.87 | 405.08 | 497.90 | 268.59 |
| Image6 | 596.22 | 502.63 | 649.62 | 506.13 | 577.17 | 438.71 | 416.50 | 315.06 |
| Image7 | 559.43 | 515.88 | 588.80 | 479.79 | 416.06 | 497.11 | 402.05 | 205.81 |
| Image8 | 574.66 | 534.87 | 605.56 | 490.35 | 459.10 | 460.86 | 413.37 | 191.21 |
| Image9 | 530.86 | 481.82 | 561.04 | 459.46 | 482.79 | 494.99 | 380.96 | 225.02 |
| Image10 | 551.99 | 510.20 | 581.30 | 477.24 | 470.10 | 492.15 | 395.99 | 219.42 |
| Image11 | 587.26 | 553.40 | 610.83 | 501.17 | 656.16 | 516.27 | 420.21 | 239.74 |
| Image12 | 591.02 | 575.80 | 602.53 | 523.58 | 655.67 | 556.51 | 421.83 | 186.14 |
| Image13 | 554.08 | 516.39 | 580.67 | 480.28 | 525.47 | 478.83 | 397.26 | 220.31 |
| Image14 | 591.28 | 568.02 | 612.41 | 515.83 | 620.85 | 513.32 | 423.20 | 209.31 |
| Image15 | 558.98 | 511.12 | 592.28 | 475.45 | 542.81 | 529.32 | 402.31 | 233.26 |
| Image16 | 569.64 | 532.62 | 599.15 | 487.60 | 533.49 | 454.94 | 409.34 | 214.64 |
| Image17 | 577.52 | 547.20 | 604.32 | 495.06 | 628.77 | 513.75 | 414.80 | 175.74 |
| Image18 | 559.06 | 515.28 | 590.02 | 476.60 | 616.25 | 497.20 | 401.90 | 217.30 |
| Image19 | 630.32 | 599.01 | 653.79 | 549.54 | 551.43 | 525.36 | 453.59 | 188.98 |
| Image20 | 556.21 | 547.05 | 580.66 | 498.62 | 671.29 | 526.30 | 397.57 | 193.88 |
| Image21 | 553.08 | 551.49 | 582.07 | 491.57 | 552.13 | 478.36 | 396.91 | 192.50 |
| Image22 | 494.37 | 422.55 | 526.43 | 423.32 | 520.51 | 467.76 | 354.39 | 273.38 |
| Image23 | 445.43 | 283.34 | 488.87 | 377.22 | 553.36 | 435.49 | 315.35 | 480.95 |
| Image24 | 533.35 | 471.65 | 567.25 | 457.38 | 490.79 | 524.81 | 383.16 | 234.57 |
| Image25 | 524.22 | 476.98 | 556.53 | 449.86 | 492.65 | 416.74 | 376.75 | 235.05 |
| Average MSE | 565.41 | 517.84 | 596.96 | 487.69 | 550.21 | 488.11 | 403.82 | 229.92 |

Table.2. Peak Signal to Noise Ratio of the Proposed Gamma Corrected Gaussian Filtering Framework and the Traditional Filters

| Sample Image | PSNR of Existing Spatial Domain and frequency Domain Filters | | | | | | | PSNR of proposed Filter |
|---|---|---|---|---|---|---|---|---|
| | Mean Filter | Weighted Averaging Filter | Minimum Filter | Maximum Filter | Median filter | Wiener Filter | Gaussian Filter | |
| Image1 | 20.45 | 20.63 | 20.31 | 21.01 | 14.57 | 14.75 | 21.91 | 24.81 |
| Image2 | 20.91 | 21.33 | 20.70 | 21.56 | 14.98 | 15.32 | 22.36 | 24.64 |
| Image3 | 20.53 | 20.61 | 20.45 | 21.05 | 14.36 | 15.07 | 22.00 | 25.38 |
| Image4 | 20.50 | 20.71 | 20.31 | 21.17 | 14.65 | 14.75 | 21.94 | 25.09 |
| Image5 | 19.49 | 20.55 | 18.88 | 20.34 | 14.14 | 14.31 | 21.15 | 23.83 |
| Image6 | 20.37 | 21.11 | 20.00 | 21.08 | 14.75 | 14.82 | 21.93 | 23.14 |
| Image7 | 20.65 | 21.01 | 20.43 | 21.32 | 14.87 | 14.91 | 22.07 | 24.99 |
| Image8 | 20.53 | 20.84 | 20.30 | 21.22 | 14.78 | 14.78 | 21.96 | 25.31 |
| Image9 | 20.88 | 21.30 | 20.64 | 21.50 | 15.15 | 15.13 | 22.36 | 24.60 |
| Image10 | 20.71 | 21.05 | 20.48 | 21.34 | 14.97 | 14.92 | 22.15 | 24.71 |
| Image11 | 20.44 | 20.70 | 20.27 | 21.13 | 14.54 | 14.67 | 21.89 | 24.32 |
| Image12 | 20.41 | 20.52 | 20.33 | 20.94 | 14.40 | 14.79 | 21.87 | 25.43 |
| Image13 | 20.69 | 21.00 | 20.49 | 21.31 | 14.85 | 14.95 | 22.14 | 24.70 |
| Image14 | 20.41 | 20.58 | 20.26 | 21.00 | 14.47 | 14.68 | 21.86 | 24.92 |
| Image15 | 20.65 | 21.04 | 20.40 | 21.35 | 15.03 | 14.84 | 22.08 | 24.45 |
| Image16 | 20.57 | 20.86 | 20.35 | 21.25 | 14.83 | 14.79 | 22.00 | 24.81 |
| Image17 | 20.51 | 20.74 | 20.31 | 21.18 | 14.65 | 14.88 | 21.95 | 25.68 |
| Image18 | 20.65 | 21.01 | 20.42 | 21.34 | 14.87 | 14.91 | 22.08 | 24.76 |
| Image19 | 20.13 | 20.35 | 19.97 | 20.73 | 14.23 | 14.46 | 21.56 | 25.36 |
| Image20 | 20.67 | 20.75 | 20.49 | 21.15 | 14.56 | 15.06 | 22.13 | 25.25 |
| Image21 | 20.70 | 20.71 | 20.48 | 21.21 | 14.60 | 14.95 | 22.14 | 25.28 |
| Image22 | 21.19 | 21.87 | 20.91 | 21.86 | 15.52 | 15.41 | 22.63 | 23.76 |
| Image23 | 21.64 | 23.60 | 21.23 | 22.36 | 16.50 | 15.26 | 23.14 | 21.30 |
| Image24 | 20.86 | 21.39 | 20.59 | 21.52 | 14.92 | 15.28 | 22.29 | 24.43 |
| Image25 | 20.93 | 21.34 | 20.67 | 21.60 | 14.92 | 15.53 | 22.37 | 24.41 |
| **Average PSNR** | **20.61** | **21.02** | **20.38** | **21.26** | **14.80** | **14.92** | **22.07** | **24.61** |

The Table.1 compares the MSE rate of the proposed GCGF framework against the typical spatial domain and frequency domain filters such as, mean, weighted-averaging, Gaussian, minimum, maximum, median, and Wiener filters. The MSE value is shown for 25 randomly chosen chest X-ray dataset images and the average MSE value for the output images is also shown.

The Table.2 registers the PSNR rate of the same set of chosen traditional filters and the proposed GCGF framework. The table also lists the average PSNR value of 25 images.

# 7. CONCLUSION

Sensitive medical images need much care to deliver without noise distortion. The proposed Gamma Corrected Gaussian Filtering framework decreases the noise present in COVID-19 chest X-ray pictures and adjusts the image pixels' illumination. The GCGF framework increases the quality of the X-ray images by reducing the quantum noise. The GCGF framework is compared with standard techniques and results ensures its efficacy. The performance of the filters are evaluated using the metrics MSE and PSNR; which prove that, the GCGF framework attains a higher level of PSNR and lower MSE than the standard filters. Thus ensures the image with enhanced visual quality.

The traditional filtering methods analyzed in this article is used to pre-process the datasets with fewer number of test images. To cope up with the evolving technologies, the deep learning autoencoder based filtering techniques can be explored in future for pre-processing the image datasets with a large number of images.

# REFERENCES

[1] Anirban Saha and P.S.J. Kumar, "Improved Digital Image Processing Based Detection for Alzheimer's Disease using MATLAB", *International Journal of Advances in Arts, Sciences, and Engineering*, Vol. 3, No. 6, pp. 1-14, 2015.

[2] D. Umamaheswari and S. Geetha, "Review on Image Segmentation Techniques Incorporated with Machine Learning in the Scrutinization of Leukemic Microscopic Stained Blood Smear Images", *Proceedings of International Conference on Computational Vision and Bio-Engineering*, pp. 158-163, 2018.

[3] Duraiswamy Umamaheswari and Shanmugam Geetha, "A Framework for Efficient Recognition and Classification of Acute Lymphoblastic Leukemia with a Novel Customized-Knn Classifier", *Journal of Computing and Information Technology*, Vol. 26, No. 2, pp. 131-140, 2018.

[4] D. Umamaheswari and S. Geetha, "Segmentation and Classification of Acute Lymphoblastic Leukemia Cells Tooled with Digital Image Processing and ML Techniques", *Proceedings of International Conference on Intelligent Computing and Control* Systems, pp. 1336-1341, 2018.

[5] Youlian Zhu and Cheng Huang, "An Improved Median Filtering Algorithm for Image Noise Reduction", *Physics Procedia*, Vol. 25, pp. 609-616, 2012.

[6] R. Silpasai, S.V. Raghavendra Kommuri, H. Singh, A. Kumar and L.K. Balyan, "Optimal Gamma Correction based Gaussian Unsharp Masking Framework for Enhancementof Histopathological Images", *Proceedings of International Conference on Communication and Signal Processing*, pp. 460-464, 2019.

[7] Himanshu Singh, Anil Kumar, L.K. Balyan and G.K. Singh, "Swarm Intelligence Optimized Piecewise Gamma Corrected Histogram Equalization for Dark Image Enhancement", *Computers and Electrical Engineering*, Vol. 70, pp. 462-475, 2018.

[8] Shipra Suman, Fawnizu Azmadi Hussin, Aamir Saeed Malik, Nicilas walter, Khean Lee Goh, Ida Hilmi and Shiaw hooi Ho, "Image Enhancement Using Geometric Mean Filter and Gamma Correction for WCE Images", *Proceedings of International Conference on Neural Information Processing*, pp. 26-34, 2014.

[9] Sheikh Tania and Raghad Rawaida, "A Comparative Study of Various Image Filtering Techniques for Removing various Noisy pixels in Aerial Image", *International Journal of Signal Processing, Image Processing, and Pattern Recognition*, Vol. 9, No. 3, pp. 113-124, 2016.

[10] Rafael C. Gonzalez and Richard E. Woods, "*Digital Image Processing*", 3rd Edition, Pearson Publications, 2012.

[11] Youlian Zhu and Cheng Huang, "An Improved Median Filtering Algorithm for Image Noise Reduction", *Physics Procedia*, Vol. 25, pp. 609-616, 2012.

[12] Jebamalar Leavline and Asir Antony, "Salt and Pepper Noise Detection and Removal in Gray Scale Images: An Experimental Analysis", *International Journal of Signal Processing, Image Processing and Pattern Recognition*, Vol. 6, No. 2, pp. 343-352, 2013.

[13] Ruchika Chandel and Gaurav Gupta, "Image Filtering Algorithms and Techniques: A Review", *International Journal of Advanced Research in Computer Science and Software Engineering*, Vol. 3, No. 10, pp. 1-16, 2013.

[14] E. Vincent, "An Experimental Evaluation of Wiener Filter Smoothing Techniques Applied to Under-Determined Audio Source Separation", *Proceedings of International Conference on Latent Variable Analysis and Signal Separation*, pp. 157-164, 2010.

[15] Duraiswamy Umamaheswari and Shanmugam Geetha, "Multi-class ECOCAMD Classifier in Classification of the types of White Blood Cells", *International Journal of Advance Science and Technology*, Vol. 29, No. 3, pp. 3834-3849, 2020.

[16] S. Somal, A. Luhach and J. Kosa, "Image Enhancement Using Local and Global Histogram Equalization Technique and Their Comparison", *Proceedings of 1st International Conference on Sustainable Technologies for Computational Intelligence Advances in Intelligent Systems and Computing*, pp. 1-12, 2010.

[17] Joseph Paul Cohen, Paul Morrison and Lan Dao, "Covid-19 Image Data Collection", *Proceedings of International Conference on Image and Video Processing*, pp. 111-118, 2020.

[18] Prashan Premaratne and Malin Premaratne, "Image Matching using Moment Invariants", *Neurocomputing*, Vol. 137, pp. 65-70, 2014, pp 65-70.

[19] Z. Kotevski Z. and P. Mitrevski, "Experimental Comparison of PSNR and SSIM Metrics for Video Quality Estimation", *Proceedings of International Conference on Information and Communications*, pp. 23-27, 2009.

[20] A. Hore and D. Ziou, "Image Quality Metrics: PSNR vs. SSIM", *Proceedings of International Conference on Pattern Recognition*, pp. 2366-2369, 2010.